Superposition and higher-order spacing ratios in random matrix theory with application to complex systems

Udaysinh T. Bhosale ◉*

Department of Physics, National Institute of Technology, Nagpur 440010, India
and Physical Research Laboratory, Navrangpura, Ahmedabad 380009, India

The statistical properties of spectra of quantum systems within the framework of random matrix theory are widely used in many areas of physics. These properties are affected if two or more sets of spectra are superposed, resulting from the discrete symmetries present in the system. The superposition of spectra of m such circular orthogonal, unitary, and symplectic ensembles are studied numerically using higher-order spacing ratios. For given m and the Dyson index β, the modified index β' is tabulated whose nearest-neighbor spacing distribution is identical to that of k-th order spacing ratio. For the case of $m = 2$ ($m = 3$) in the Circular Orthogonal Ensemble (Circular Unitary Ensemble) a scaling relation between β' and k is given. For COE, it is conjectured that for $k = m + 1$ ($m \geqslant 2$) and $k = m - 3$-th ($m \geqslant 5$) order spacing ratio distribution the β' is $m + 2$ and $m - 4$, respectively, whereas in the case of the Circular Symplectic Ensemble, for $k = m + 1$ ($m \geqslant 2$) and $k = m - 1$-th ($m \geqslant 3$) the β' is $2m + 3$ and $2(m - 2)$, respectively. We also conjecture that for given m (k) and β, the sequence of β' as a function of k (m) is unique. Strong numerical evidence in support of these results is presented. These results are tested on complex systems like the measured nuclear resonances, quantum chaotic kicked top and spin chains.

I. INTRODUCTION

Random matrix theory (RMT) has been successfully applied to study the spectral fluctuations in various complex quantum systems [1–9]. These include spin chains from condensed matter physics [10–14], nuclear physics [1,2,15], chaotic billiards [16,17], etc. These fluctuations are used to characterize various phases of these systems, for example, thermal or localized phase of spin chains [12–14,18], integrable to chaotic limit of the underlying classical system [19,20], etc. For correct characterization of the system, its spectra need to be desymmetrized [21]. If the Hamiltonian H for a given system possess an additional symmetry S, i.e., $[H, \hat{S}] = 0$, where $\hat{S}$ is the operator corresponding to S, then the eigenvalues get superposed. This can lead to entirely different fluctuation properties failing to characterize the system [8,21–27]. Due to symmetry S the H becomes block diagonal in the basis formed by the eigenfunctions of S, i.e., $H = H_1 \oplus H_2 \oplus \ldots \oplus H_m$. Here, m denotes the number of nondegenerate eigenvalues of S. Thus, due to the symmetry S, in the spectra of H, the eigenvalues from different blocks get superposed. Symmetries also have played an important role in our understanding of many areas of physics [28–31], mathematics [31,32], biology [33], etc. The importance of symmetries can be understood from the works of Emmy Noether, where she has related continuous symmetry and conservation laws in her famous theorem [34,35]. Symmetries have also played an important role in the RMT [7,8]. This goes back to Wigner who defined a class of Gaussian random

matrix ensembles to understand the fluctuations in the nuclear spectra. The class of ensemble one uses depends on the symmetry present in the system. In RMT, the spectral fluctuations are modeled using the most popular measure, namely, the nearest-neighbor (NN) level spacings, $s_i = E_{i+1} - E_i$, where E_i, $i = 1, 2, \ldots$ are the eigenvalues of the Hamiltonian H. Wigner surmised that in time-reversal invariant systems without a spin degree of freedom, these spacings are distributed as $P(s) = (\pi/2)s \exp(-\pi s^2/4)$, which indicates the level repulsion. For these systems, the statistical properties of the spectra are modeled correctly by the Gaussian Orthogonal Ensemble (GOE) having Dyson index $\beta = 1$. Other ensembles that are used commonly in RMT are Gaussian unitary ensemble (GUE) and Gaussian symplectic ensemble (GSE) having Dyson index $\beta = 2$ and 4, respectively, having applications to various fields [4,36]. In this work, the circular class of ensembles has been studied [7] and based on previous studies our results can be extended to Gaussian ensembles for large matrix dimensions under certain conditions as explained in Sec. II [7,8,21,37–39]. The symmetries that are used in defining respective Gaussian ensembles are the same for those of circular ensembles. Indices $\beta = 1$, 2, and 4 correspond to Dyson's threefold way and have played an important role in physics. Matrix representation for these indices was given in the initial development of RMT. But these ensembles are valid and exits for continuous parameter $\beta \in (0, \infty)$ and a tridiagonal random matrix model have been defined for them [40]. It has been used recently in the study of level statistics of many-body localization for $\beta \in (0, 1]$ [41,42]. The index β is interpreted as the inverse temperature of $T = 1/\beta$ in the RMT literature. In 1984, Bohigas, Giannoni, and Schmidt conjectured that quantum chaotic systems display NN level statistics

*udaybhosale0786@gmail.com

consistent with that of an appropriately chosen random matrix ensemble [9,16]. This conjecture is supported by many theoretical studies [43–45]. Due to the additional symmetry S, which may not be known *a priori*, the eigenvalues from different blocks get superposed. This results in level clustering of NN and one obtains their spacings distribution to be Poissonian [8,9,46–48], $P(s) = \exp(-s)$, which also corresponds to the NN spectral fluctuations of integrable systems known as Berry and Tabor's conjecture [49]. This implies that to study the genuine spectral correlations, eigenvalues must be drawn from the same subspace. Motivated by the works of Wigner, Dyson introduced a new class of ensembles of random matrices known as circular β-ensembles which are measures in the spaces of unitary matrices [50]. They have played important roles in RMT. The Dyson index $\beta = 1, 2$, and 4 corresponds to the Circular Orthogonal Ensemble (COE), the Circular Unitary Ensemble (CUE), and the Circular Symplectic Ensemble (CSE), respectively. These ensembles have found applications in the scattering from a disordered cavity [7], condensed matter, and optical physics [4]. The algorithm for generating these ensembles numerically is nontrivial compared with that of Gaussian ensembles and is given in Ref. [51]. Similar to the Gaussian β-ensemble, the circular β-ensemble is also defined for continuous parameter $\beta \in (0, \infty)$, and a corresponding tridiagonal model is defined for them [24,52]. Previous studies have shown connections within ensembles corresponding to $\beta = 1, 2$, and 4. A theorem that relates the properties of the CUE and COE has been conjectured in Ref. [22] and later proved by Gunson [23]. It states that the alternate eigenvalues obtained after superposition of spectra of two matrices ($m = 2$ as per our notation) of the same dimension from COE belong to that of CUE. A similar theorem relating properties of COE and CSE were proved in Ref. [53]. It states that the alternate eigenvalues of an even-dimensional COE belong to that of CSE. Thus, these two theorems together state that all the statistical properties of the three ensembles are derivable from that of COE alone [53]. In fact, these two theorems hold at the level of joint probability distribution function (jpdf). As a corollary of these theorems, one can also say that level fluctuations of CUE and CSE can be obtained using COE. It is also conjectured that similar relationships hold true for Gaussian ensembles of infinite dimensions, in which the GOE underlies the GUE and GSE [38,39]. There are recent studies where higher-order spacing ratios are studied in the superposed spectra [21]. There it is shown that when the m number of COE spectra is superposed then the distribution of the m-th order spacing ratios is the same as that of NN spacing ratios of the circular ensemble with modified Dyson index m. (The definition of higher-order spacing ratios will be given in detail in Sec. II.) This result is then used to find symmetries in various physical systems like spin chains, quantum billiards, and experimentally measured nuclear resonances. Similarly in Ref. [25], the distribution of NN spacing as well as the NN spacings ratio is studied in Gaussian ensembles when discrete symmetries are present with no restriction of their numbers. These results are then applied to quantum many-body systems, anyonic chains to periodically driven spin systems, and quantum clock models. It can be seen that only the special cases of spacings and their ratios for given m are studied in Refs. [21,25]. In this paper, our main aim is to study k-th

higher-order spacing ratios for given m superpositions for each of the COE, CUE, and CSE ensembles. There will be no restriction on the value of k as it was in Ref. [21] where $k = m$. We will be validating our COE results by testing them on the physical model like the quantum kicked top (QKT), experimentally measured nuclear resonances, and spin Hamiltonian. Our results can also be used as a stringent test for studying symmetries in other systems. The structure of the paper is as follows: In Sec. II, the definitions of various quantities, namely, the NN spacing ratios and higher-order spacing ratios are given. Previous studies from RMT and other fields using these definitions are presented. In Sec. III, our results using the higher-order spacing ratios of superposition of COEs are presented. In Sec. IV, we show the application of these results to the physical systems. In Sec. V (Sec. VI), we present results on higher-order spacing ratios of superposition of CUEs (CSEs). In Sec. VII, various numerical methods used in this paper in support of our results are presented. In Sec. VIII, a summary of the results and conclusion is given.

II. PRELIMINARIES

For the study of the spacing distribution, one needs to unfold the spectra which removes the system-dependent spectral features, i.e., the average part of the density of states (DOS) [3,6,8,49,54]. This procedure is nonunique and cumbersome in many cases which can give misleading results [55]. This difficulty can be solved by using the NN spacing ratios [18], i.e., $r_i = s_{i+1}/s_i$, $i = 1, 2, \ldots$, since it is independent of the local DOS and thus does not require unfolding. The distribution of r_i, $P(r)$ has been obtained for Gaussian ensembles and is given as follows [56,57]:

$$P(r, \beta) = \frac{1}{Z_\beta} \frac{(r + r^2)^\beta}{(1 + r + r^2)^{(1+3\beta/2)}}, \quad \beta = 1, 2, 4, \quad (1)$$

where Z_β is the normalization constant that depends on β. This quantity has found many applications, like the numerical investigation of many-body localization [18,41,58–62], localization in constrained quantum system [63], and quantifying the distance from integrability on finite size lattices [26,64–67] and to study localization transition in Lévy matrices [68], symmetries in various complex systems [21,25], the degree of chaoticity in different random matrix models [69], quantum chaos in Sachdev-Ye-Kitaev models [70–72], and quantum field theory [73]. Variations of the spacing ratios have been studied in the recent past [57,74–76] including generalization to complex eigenvalues [77]. In this work, the nonoverlapping k-th order spacing ratio is considered, where no eigenvalue is shared between the spacings of numerator and denominator, and is defined as follows:

$$r_i^{(k)} = \frac{s_{i+k}^{(k)}}{s_i^{(k)}} = \frac{E_{i+2k} - E_{i+k}}{E_{i+k} - E_i}, \quad i, k = 1, 2, 3, \ldots. \quad (2)$$

This ratio has been used to study higher-order fluctuation statistics in the Gaussian [37], circular [37], and Wishart ensembles [78], and a scaling relation is given as follows:

$$P^k(r, \beta, m = 1) = P(r, \beta'), \quad \beta \geqslant 1$$
$$\beta' = \frac{k(k+1)}{2}\beta + (k-1), \quad k \geqslant 1. \quad (3)$$

TABLE I. Tabulation of higher-order indices β' for various k and β using Eq. (3).

k	$\beta = 1$	$\beta = 2$	$\beta = 3$	$\beta = 4$	$\beta = 5$	$\beta = 6$	$\beta = 7$
1	1	2	3	4	5	6	7
2	4	7	10	13	16	19	22
3	8	14	20	26	32	38	44
4	13	23	33	43	53	63	73
5	19	34	49	64	79	94	109
6	26	47	68	89	110	131	152
7	34	62	90	118	146	174	202
8	43	79	115	151	187	223	259

TABLE II. Tabulation of higher-order indices β' for various k and superposition of m COEs each having dimension $N = 8400$.

k	$m = 2$ β'	$m = 3$ β'	$m = 4$ β'	$m = 5$ β'	$m = 6$ β'	$m = 7$ β'
1	0	0	0	0	0	0
2	2	1.25	1	1	0.75	0.75
3	4	3	2.5	2	2	2
4	7	5	4	3.5	3	3
5	10	7.5	6	5	5	4
6	14	10	8	7	6	6
7	18	13	11	9	8	7
8	23	17	13	12	10	9
9	28	20	16	14	12	11
10	34	24	20	17	15	13
11	40	29	23	20	17	16
12	47	33	27	23	20	18
13	54	38	31	26	23	21
14		43	35	30	26	23
15		49	39	33	29	26
16			44		32	29
17						32
18						35
19						39
20						42

It tells that the distribution of k-th order spacing ratio for a given β-ensemble is the same as that of NN spacing ratios of $\beta'(> \beta)$ ensemble. It has been applied successfully to various physical systems like spin chains, chaotic billiards, Floquet systems, observed stock market, etc. [37,78,79]. It was also used recently to find the symmetries in complex systems [21]. It should be noted here that the results obtained for the case $k = 1$ are found to be universal since it does not depend on the local DOS, whereas for $k > 1$ one needs to be careful since the DOS, which changes from ensemble to ensemble, can affect the distribution of $r_i^{(k)}$. For example, in the case of circular ensembles (introduced in Sec. III), the DOS is uniform; for Gaussian ensembles, it is Wigner's semicircle; whereas for the Wishart ensemble, it is given by Marchenko-Pastur distribution [8]. Thus, only in the case of circular ensembles, DOS will not affect the higher-order spacing ratios. In the case of physical systems, DOS can be different even if their NN fluctuation properties are explained by the same kind of RMT ensemble [2,12–14,26,27,37,80]. Thus, the results for $k > 1$ cannot be claimed to be universal that easily. But evidence from Ref. [37] (see Fig. 5 therein) suggests that for a given k, if the matrix dimension is increased large enough, which will depend on the RMT ensemble and the physical system under consideration, then our RMT results can be applied to them. This means that the effects of nonuniform density can be minimized by increasing the matrix dimension for a given value of k. This will also be demonstrated in Sec. IV, where we apply the RMT results to the physical system of spin chain. Recently, the same relation between the higher-order and the NN spacing distributions had been shown rigorously, which is tested on random spin systems and nontrivial zeros of the Riemann zeta function [12,39,81–84]. In Ref. [21] (as explained in the Introduction), the distribution of the m-th order spacing ratios after superposing the spectra of m COEs is studied. It is shown to be converging to the distribution of the NN spacing ratios $P(r, \beta')$ with $\beta' = m$, i.e.,

$$P^k(r, 1, m) = P(r, \beta'), \text{ where } \beta' = k = m. \quad (4)$$

Equation (3) is tabulated for few values of β and k in Table I. It can be observed from the $\beta = 1$ series in Table I that the $\beta = 4$ series appears at its even places. This is because the relation between COE and CSE exists at the level of the jpdf of the eigenvalues [22,23] as discussed in the Introduction. This observation plays an important role in further analysis in the subsequent parts of this paper. The special case of the Eq. (3)

for $0 \leqslant \beta \leqslant 1$ is given in Refs. [85,86] at the level of the joint probability distribution of eigenvalues. There, it is shown that the jpdf of every k-th eigenvalue in certain β-ensembles with $\beta = 2/k$ is equal to that of another β-ensemble with $\beta = 2k$. Based on numerical simulations, the results of our work will now be presented.

III. SUPERPOSITION AND HIGHER-ORDER SPACING RATIOS IN COE

In this work, the main object of study is the circular β ensembles. The jpdf is given as follows:

$$Q_{N,\beta}[\{\theta_i\}] = C_{N,\beta} \prod_{k>j}^{N} |\exp(i\theta_j) - \exp(i\theta_k)|^{\beta}, \quad (5)$$

where N is the dimension and $C_{\beta,N} = (2\pi)^{-N}\{\Gamma(1 + \beta/2)\}^N\{\Gamma(1 + N\beta/2)\}^{-1}$ is the normalization constant [7,8]. The eigenvalues θ_i are distributed uniformly on the unit circle and display level repulsion, characterized by $\beta \geqslant 0$ [8]. Larger the value of β larger is the repulsion. It can be seen that if $\beta = 0$ is put in the jpdf all the eigenvalues are independent and thus uncorrelated. For such eigenvalues the level statistics follow a Poisson law. In this section, we consider the superposition of $m \geqslant 2$ number of COEs and study its nonoverlapping k-th order spacing ratio distribution $P^k(r, \beta, m)$. For COE, $\beta = 1$ is taken and is used in modeling Hamiltonians which possess time-reversal symmetry and no half-integer spin [8]. This is then related with the NN spacing ratio distribution $P(r, \beta')$ for $\beta' > \beta$. For given m and k we tabulate the value of β' for which both these distributions are very close to each other numerically. These values are given in Table II for $m = 2$ to 7 and various values of k. It can be seen that
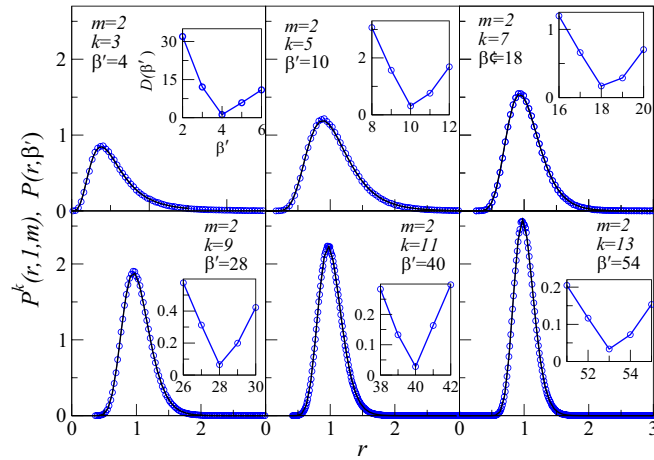
FIG. 1. Distribution of the k-th order spacing ratios (circles) for a superposition of $m = 2$ COE spectra. The dimension of the matrices is $N = 8400$. The solid curve corresponds to $P(r, \beta')$ as given in Eq.(1) with β' given in Table II. The insets show D as a function of β'.

TABLE III. Tabulation of higher-order indices β' for various k and superposition of m CUEs, each having dimension $N = 10000$.

k	$m = 2$ β'	$m = 3$ β'	$m = 4$ β'	$m = 5$ β'
1	0	0	0	0
2	3	1.5	1	0.75
3	6	4	3	2
4	11	7	6	4
5	15	11	8	7
6	22	15	11	10
7	28	20	15	13
8	36	25	20	16
9	43	31	24	20
10	55	37	29	24
11	64	44	34	28
12	75	51	40	33
13		59		
14		67		
15		76		
16		85		

except for a few, all values of β' are whole numbers (this is the case for the superposition in CUEs and CSEs, which will be discussed in subsequent parts of the paper). These results are plotted in Figs. 1–5. The insets show the $D(\beta')$ function, the minimum of which gives the best fit $P(r, \beta')$ to the numerical data $P^k(r, \beta, m)$. Its detailed definition and other numerical methods with which we find β' will be discussed in Sec. VII. We have also plotted a representative data for noninteger β' in Sec. V (see Fig. 14 later in the paper) where we have studied the superposition of CUEs. The $m = 2$ is an interesting case for which we have obtained scaling relations for even and odd values of k and β' as given below:

$$\beta' = \frac{5k}{2} - 3 + \frac{(k-2)(k-4)}{4}, \quad k = 2, 4, 6, \ldots \quad (6)$$

and

$$\beta' = 3k - 5 + \frac{(k-3)(k-5)}{4}, \quad k = 3, 5, 7, \ldots \quad (7)$$

For even k the scaling relation reduces to Eq. (3) for $\beta = 2$ by suitable change of variables as $l = k/2$ where $l = 1, 2, 3, \ldots$. This is a known result in the connection between CUE and the superposition of two COEs [22,23]. For odd k changing the variable as $q = (k - 1)/2$ then Eq. 7 reduces to a simpler form as $\beta' = q(q + 3)$ for $q = 1, 2, 3 \ldots$. It can be compared with Eq. (3) and can be seen that it does not reduce to Eq. (3) for any β. Thus, using the scaling relation in Eq. (7), no statement can be made at the level of jpdf of circular β-ensemble. Based on the results in Table II, we have given two conjectures on the lines of Eq. (4) (see Ref. [21]) at the level of spectral fluctuations. The first conjecture is as follows:

$$P^k(r, 1, m) = P(r, \beta'), \text{ for } \beta' = k + 1 = m + 2, \quad (8)$$

and $m \geqslant 2$, while the second one is as follows:

$$P^k(r, 1, m) = P(r, \beta'), \text{ for } \beta' = k - 1 = m - 4, \quad (9)$$

and $m \geqslant 5$. Our conjectures hold true for asymptotic value of N. These conjectures have appeared in Ref. [87].

IV. TESTING RMT RESULTS TO PHYSICAL SYSTEMS

In this section, we test our COE results on the physical model of the QKT, experimentally measured data of nuclear resonances and a spin Hamiltonian. Using these systems it will be shown that our results hold true for $m = 2$ case. First, we consider the model of QKT. This is a fundamental and important time-dependent model for the chaotic Hamiltonian system. This model was introduced in Ref. [19] and has been the topic of theoretical and experimental research since then [19,88–103]. It has been realized in various experiments, namely, the hyperfine states of cold atoms [92], three coupled superconducting qubits [95], and in a two-qubit NMR system [99]. This is also an important model from the perspective of RMT and quantum information. This model shows regular to chaotic behavior as a function of chaoticity parameter. Effects of the underlying phase space on various measures quantum correlations are studied [95–97,104]. For classical limit being fully chaotic, the NN fluctuations of symmetry reduced spectra of the QKT corresponds to that of COE ensemble [16,19]. QKT is characterized by an angular momentum vector $\mathbf{J} = (J_x, J_y, J_z)$ and its components obey the standard algebra of angular momentum. The unitary time evolution operator for QKT is given as follows:
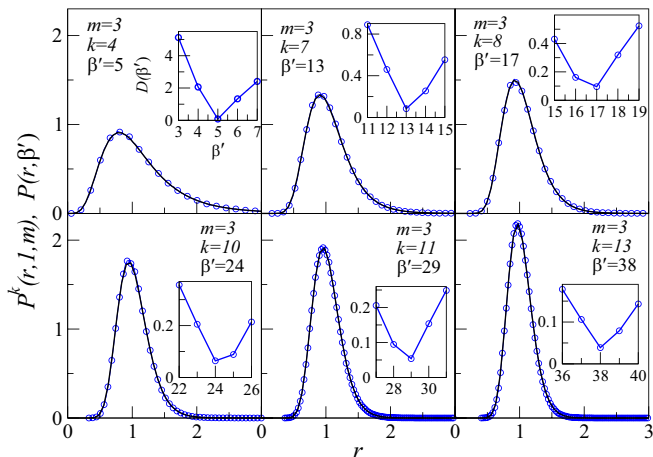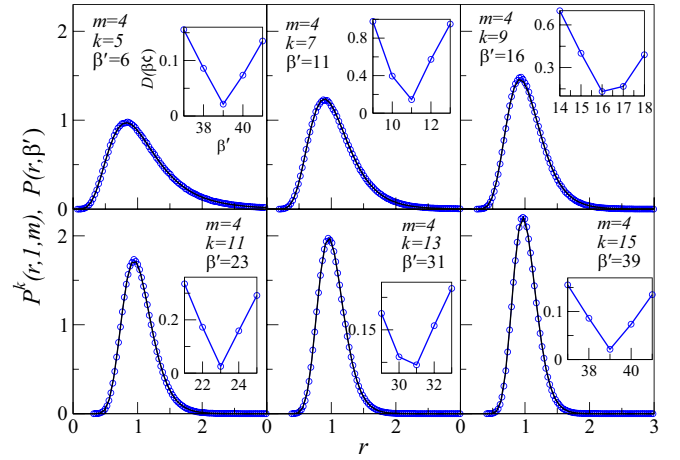
$$\widehat{U} = \exp\left(-ipJ_y\right) \exp\left(-i\frac{k}{2j}J_z^2\right). \quad (10)$$

It represents free precession of the top around the y axis with angular frequency p while the second term is periodic δ kicks applied to the top. Here, k is called as the kick strength or chaos parameter. For $k = 0$ the top is integrable and for $k > 0$ it becomes increasingly chaotic. For given j the Hilbert space dimension is equal to $2j + 1$. As discussed in Ref. [19], for $p \neq \pi/2$, the case relevant for us, there are two symmetries present in QKT, since $\widehat{U}$ commutes with the rotation operator $\hat{R}_y$ having two eigenvalues. Thus, the matrix representation of $\widehat{U}$ in the basis of R_y is block diagonal consisting of two

TABLE IV. Tabulation of higher-order indices β' for various k and superposition of m CSEs each having dimension $N = 1000$.

k	$m = 2$ β'	$m = 3$ β'	$m = 4$ β'	$m = 5$ β'	$m = 6$ β'
1	0	0	0	0	0
2	5	2	1	0.75	0.75
3	7	7	4	2.5	2
4	18	9	8	6	4
5	21	14	11	10	8
6	36	23	14	13	12
7	39	27	21	16	15
8	60	35	28	20	18
9	63	47	33	27	21
10	88	53	38	35	27
11	92	63	48	40	34
12	122	79	59	44	40

FIG. 3. The same as Fig. 1 for $m = 4$.

blocks, and their dimensions are j and $j + 1$. The large j case is relevant to us as these dimensions are very close to each other. For the fully chaotic case, the eigenvalue fluctuations of $\widehat{U}$ in each such block are found to follow COE statistics [19]. Taking these eigenvalues together and studying their higher-order spacings ratio is an ideal case for our study. We can compare them with our COE results of $m = 2$. For our study $j = 1000$ and 20 realizations for large and different values of k is taken. Thus, the dimension of the matrix $\widehat{U}$ is 2001. The dimension of two blocks when $\widehat{U}$ is written in the eigenbasis of $\hat{R}_y$ is 1000 and 1001, respectively. Thus, we can test our RMT results of $m = 2$ case of COE. The results are plotted in Figs. 6 and 7 for $k = 2$ to 13. It can be seen here that the results agree very well with the RMT results, $m = 2$ case of COE in Table II, thus implying that there are two symmetries in the QKT, which were already known *a priori* [19]. The RMT results hold true for such a large value of k due to the uniform density in both the COE ensemble and the QKT (as discussed in the Sec. II). Now, we go on to test our results to experimentally measured nuclear resonances of Tantalum (Ta^{181}) [80,105]. It is known that it belongs to the GOE and there are two symmetries present in it [80,105]. We have 434

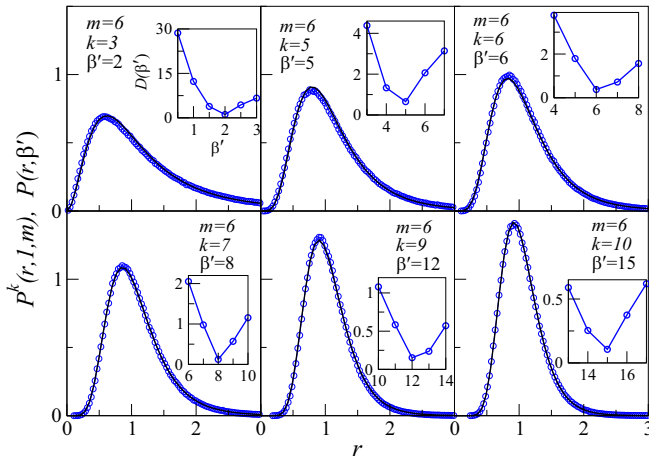such resonances and the results are plotted in Fig. 8. The value of β' is chosen such that $P(r, \beta')$ is the best fit to the data. The results are compared with $m = 2$ case of COE in Table II. It can be seen that the results hold true only for $k = 2$ and 3. From $k = 4$ onward we observe deviations from our RMT results. This is due to the nonuniversal effects in the DOS (not shown here) and the small sample size. With this example, we have tested our COE result on a GOE system with a small sample size and found the number of symmetries in it successfully. Now, a Hamiltonian corresponding to spin-1/2 chain [27,106] is considered as follows:

$$H = \sum_{i=1}^{L-1} \left[J_{xy}\left(S_i^x S_{i+1}^x + S_i^y S_{i+1}^y\right) + J_z S_i^z S_{i+1}^z \right]$$
$$+ \alpha \sum_{i=1}^{L-2} \left[J_{xy}'\left(S_i^x S_{i+2}^x + S_i^y S_{i+2}^y\right) + J_z' S_i^z S_{i+2}^z \right], \quad (11)$$

where L is the total number of sites, and the NN coupling strengths in three directions are denoted by J_{xy} and J_z (couplings in x and y directions are the same). Similarly, J_{xy}' and J_z' are the next-NN coupling strengths. For $\alpha = 0$ this Hamiltonian is integrable [21], whereas it is chaotic for $\alpha \gtrsim 0.2$

FIG. 2. The same as Fig. 1 for $m = 3$.
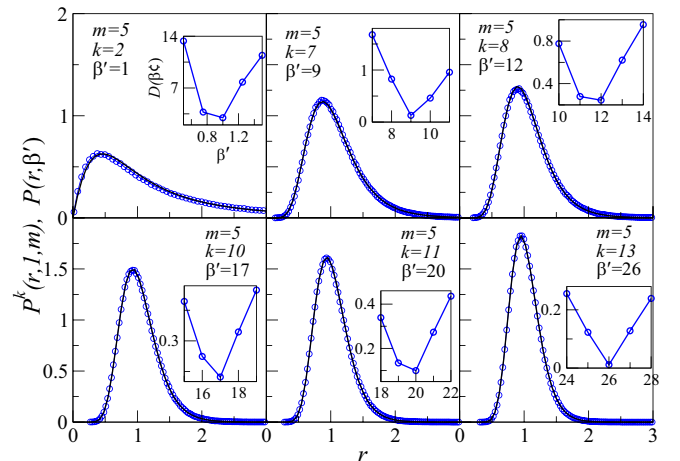
FIG. 4. The same as Fig. 1 for $m = 5$.

FIG. 5. The same as Fig. 1 for $m = 6$.

FIG. 7. The same as Fig. 6 but for $k = 8$ to 13 and $\beta' = 23, 28, 34, 40, 47, 54$.

and follows GOE statistics [27]. There are various symmetries in this model [107,108]. The first one is due to conservation of total spin in the z direction denoted as $S_z = \sum_{i=1}^{L} S_i^z$. For our work we are restricting to the case $S^z = 0$ (even L) and $S^z = -1/2$ (odd L) such that the block-matrix is of maximum possible dimension. The Hamiltonian commutes with the parity operator with eigenvalues ± 1 leading to two invariant subspaces in a given S_z block. Results for this case are plotted in Fig. 9 for odd value of L. It can be seen that our RMT results for $m = 2$ case from Table II holds true for $k = 2, 3$, and 4. For even L, the Hamiltonian also commutes with the operator corresponding to rotation symmetry with eigenvalues ± 1. Thus, in this case there will be a total of four invariant subspaces in a given S_z block. The results for this case are plotted in Figs. 10 and 11. In this case our results hold from $k = 2$ to 6 with the corresponding RMT results for $m = 4$ from Table II. Thus, our $m = 2$ and $m = 4$ the COE results agree with spin Hamiltonian having GOE statistics when there are two and four symmetries present in it, respectively. In these cases, the block-matrix dimensions are 1716 and 3432
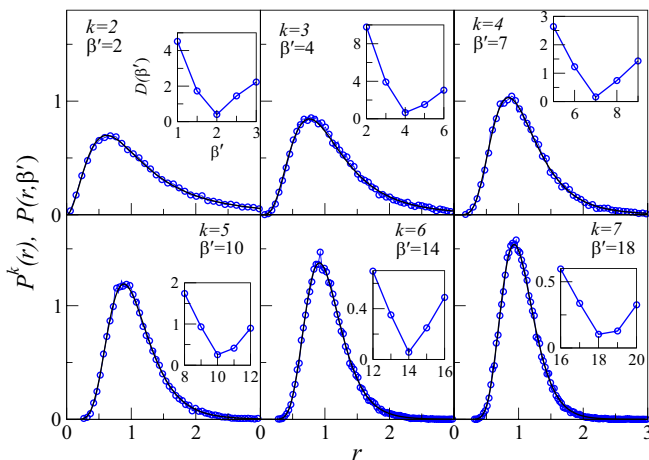
respectively. In this case also the deviations are due to the nonuniversal effects in DOS which is Gaussian in nature (not shown here). But the results seems to improve due to the increased matrix dimension.

V. SUPERPOSITION AND HIGHER-ORDER SPACING RATIOS IN CUE

In this section, we study higher-order spacings ratio in the superposition of CUEs on the lines in Section III where the superposition of COEs is studied. The CUE is used in modeling Hamiltonians that lack time-reversal symmetry [8]. The results are tabulated in Table III for $m = 2$ to 5 and various values of k. In this case also, except for a few, all values of β' are the whole number. The results are plotted in Figs. 12–14. Figure 14 shows noninteger values of β' which is found by best fit. In the case of superposing of CUEs, $m = 3$ is an interesting case for which we have obtained a scaling relation

FIG. 6. The distribution of the k-th order spacing ratios for $k = 2$ to 7 is shown for the QKT. The numerical data $P^k(r)$ (circles) are obtained from the computed eigenvalues of QKT. The solid line represents $P(r, \beta')$, with $\beta' = 2, 4, 7, 10, 14, 18$.
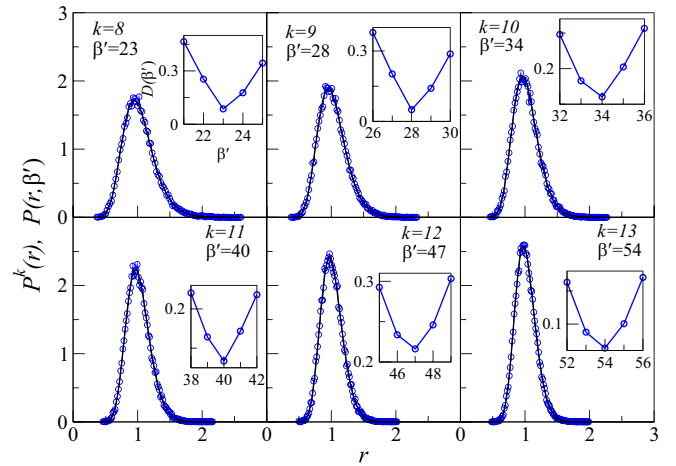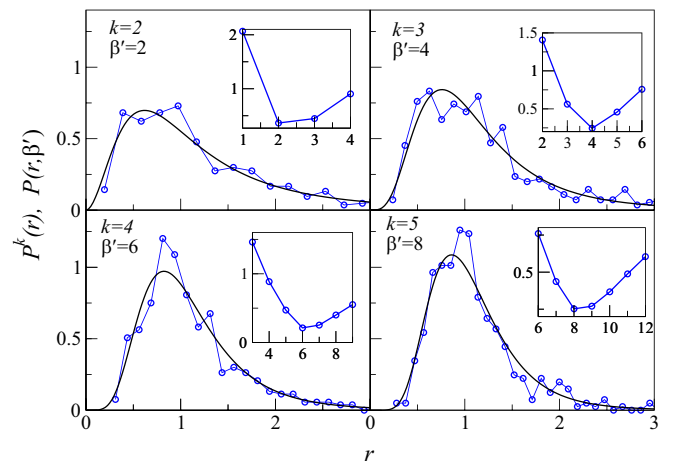

FIG. 8. The same as Fig. 6 but for experimentally measured nuclear resonances of Ta^{181}. Here, k varies from 2 to 5 while for solid curves $\beta' = 2, 4, 6,$ and 8.
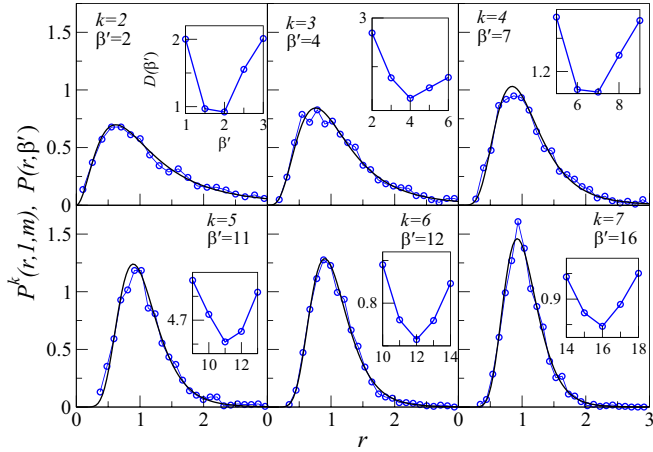
FIG. 9. The distribution of the k-th order spacing ratios for $k = 2$ to 7 is shown for the spin-1/2 chain Hamiltonian with $L = 13$ with 7 up spins, $J_{xy} = J'_{xy} = 1$, $J_z = J'_z = 0.5$ and $\alpha = 0.5$. The dimension of the block-matrix is 1716. The numerical data $P^k(r)$ (circles) are obtained from the computed eigenvalues of the Hamiltonian. The solid line represents $P(r, \beta')$, with $\beta' = 2, 4, 7, 11, 12, 16$.

for even and odd values of k and β' as given below:

$$\beta' = 4k - 9 + \frac{(k-4)(k-6)}{4}, \quad k = 4, 6, 8, \ldots \quad (12)$$

and

$$\beta' = 1 + k + \frac{5(k-3)}{2} + \frac{(k-3)(k-5)}{4}, \quad k = 3, 5, 7, \ldots . \quad (13)$$

By suitable change of variables as $l = k/2$, Eq. (12) reduces to $\beta' = l^2 + 3l - 3$ where $l = 1, 2, 3, \ldots$. While using $q = (k-1)/2$, Eq. (13) reduces to $\beta' = q^2 + 4q - 1$ where $q = 1, 2, 3 \ldots$. Comparing these series with Eq. (3), one can see that it does not reduce to Eq. (3) for any β. Thus, using the scaling relations in Eqs. (12) and (13), no statement can be made at the level of jpdf of circular β-ensemble.
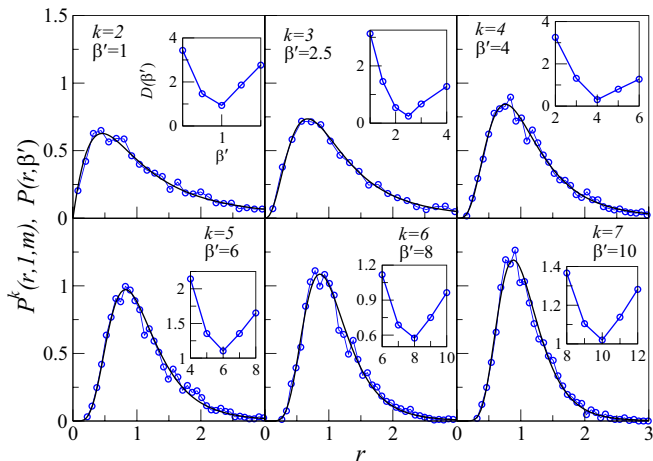

FIG. 10. The same as Fig. 9 but for $L = 14$ and $\beta' = 1, 2.5, 4, 6, 8, 10$. Here 7 spins are up and the dimension of the block-matrix is 3432.
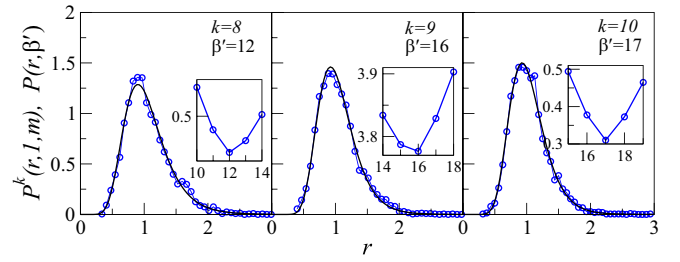

FIG. 11. The same as Fig. 10 but for $k = 8, 9, 10$ and $\beta' = 12$, 16, 17.

VI. SUPERPOSITION AND HIGHER-ORDER SPACING RATIOS IN CSE

In this section, we study higher-order spacings ratios in the superposition of CSEs on the lines in Section III. The CSE is used in modeling Hamiltonians with time-reversal symmetry and half-integer spin interaction [8,109]. The results are tabulated in Table IV for $m = 2$ to 6 and various values of k. The results are plotted in Figs. 15 and 16. In this case also, except for a few, all values of β' are whole numbers. Based on the results in Table IV, we have given two conjectures at the level of spectral fluctuations. The first conjecture is as follows:

$$P^k(r, 4, m) = P(r, \beta'), \text{ for } \beta' = 2k + 1 = 2m + 3, \quad (14)$$

and $m \geqslant 2$, while the second one is as follows:

$$P^k(r, 4, m) = P(r, \beta'), \text{ for } \beta' = 2(k-1) = 2(m-2), \quad (15)$$

and $m \geqslant 3$. Our conjectures hold true for asymptotic value of N. Although we are able to find scaling relations for only a few cases, for given m one can compare the sequence of β' as a function of k with that of $m' \neq m$, within and across Tables II–IV. It can be seen that these sequences are unique for given m and the type of ensemble considered. One can also see that this is an increasing sequence on the lines of the earlier
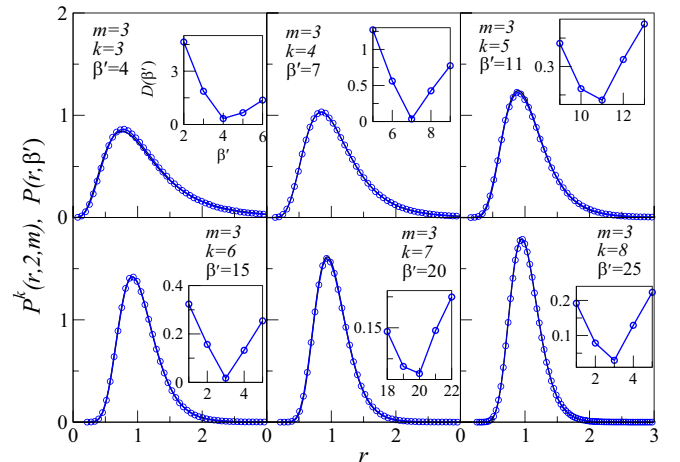

FIG. 12. Distribution of the k-th (3 to 8) order spacing ratios (circles) for a superposition of $m = 3$ CUE spectra. The dimension of the matrices is $N = 10000$. The solid curve corresponds to $P(r, \beta')$ as given in Eq. (1) with β' given in Table III. The insets show D as a function of β'.
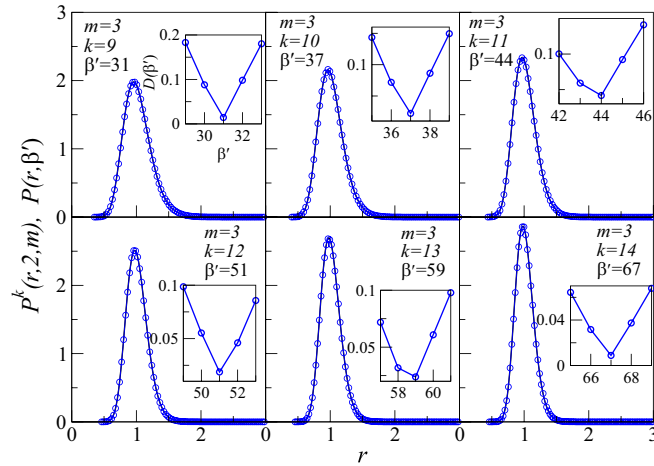
FIG. 13. The same as Fig. 12 but for $k = 9$ to 14 with corresponding β' given in Table III.

result in Eq. (3) from Refs. [37,78]. With this observation, we would like to conjecture that for a given number of symmetries m and the Dyson index β of the circular ensemble or a quantum chaotic system, the sequence of β' is an increasing function of k and completely characterizes the ensemble or the system uniquely. Similarly, for given k one can compare the sequence of β' as a function of m with that of $k' \neq k$, within and across Tables II–IV. Also, the sequences are unique for given k and decreasing. Thus, with this observation, we would like to conjecture that for given k and the Dyson index β, the sequence of β' is decreasing as a function of m and is unique. This can be interpreted physically as follows: The level repulsion present in the eigenvalues characterized by β' for given m and k is reduced as m is increased and is reflected in the reduction of the new value of β'. The implication of this conjecture is that for given β, k, and $m \to \infty$ we will see $\beta' \to 0$. It can be seen easily that one conjecture does not imply the second one. Proving our results mathematically is challenging but we give an intuitive argument for the last conjecture. We know that NN as well as the k-th eigenvalues in circular or Gaussian spectra repel each other [7]. It has also been established mathematically (analytically and numerically) that when two same-dimensional COE/GOE spectra are superposed. the NN don't repel each other (level clustering) in the limit of matrix dimensions tending to infinity, which results in their spacings distribution to be Poissonian [8,9,46–48]. In other words, before superposition,
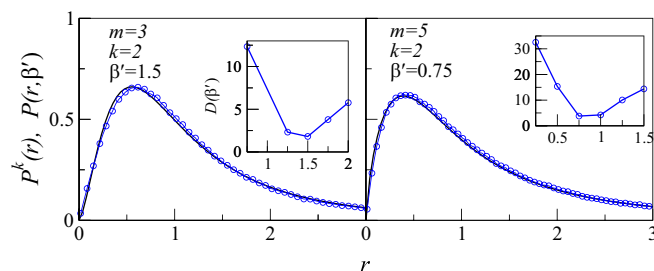
the level repulsion present (characterized by $\beta = 1$) has now vanished after superposition (characterized by $\beta = 0$). And this is what is also observed in our last conjecture, i.e., for given k and m the value of β' (characterizing the repulsion between the k-th eigenvalues) reduces as m is increased. In most of the cases we studied here, although not guaranteed, these reductions are integer number. The special case of our conjecture where $k = 1$, $N = 2$, and $m \to \infty$ is shown to have NN spacing distribution as Poissonian in Ref. [46].

VII. NUMERICAL METHODS

Now, various numerical pieces of evidence supporting our results are presented. These best fits are checked with the numerical data quantitatively. As a numerical check for our claims, analysis using Eq. (3) for $P(r, \beta')$ is carried out, where no fitting parameter is involved. For this, the difference between the cumulative distributions is numerically found and defined as follows:

$$D(\beta') = \sum_i \left| F_{\text{obs}}^k(r_i, \beta, m) - F(r_i, \beta') \right|, \quad (16)$$

where $F_{\text{obs}}^k(r, \beta, m)$ and $F(r, \beta')$ denote cumulative distribution functions corresponding to the observed histogram $P_{\text{obs}}^k(r, 1, m)$ and the numerical fit or the postulated function $P(r, \beta')$, respectively. This definition has been used in

TABLE V. The overlap probability p and the maximum absolute difference d for the results on the superposition of COEs for $m = 2, 3, 4$, and various k's.

k	$m = 2$ p, d	k	$m = 3$ p, d	k	$m = 4$ p, d
3	0.983,0.004153	3	0.992,0.00085	2	0.991,0.00164
5	0.986,0.003421	4	0.991,0.00117	4	0.991,0.00156
7	0.989,0.002506	6	0.994,0.00057	5	0.992,0.00116
9	0.994,0.001173	7	0.989,0.00246	6	0.995,0.00081
11	0.996,0.000651	8	0.988,0.00268	7	0.988,0.003263
13	0.993,0.001836	9	0.994,0.00105	8	0.995,0.00079
		10	0.988,0.0023	9	0.986,0.003078
		11	0.995,0.0014	11	0.996,0.000431
		12	0.995,0.00077	13	0.994,0.001768
		13	0.994,0.00077	15	0.996,0.000466

FIG. 14. The same as Fig. 12 but for $k = 2$, $m = 3$ and 5 with corresponding noninteger values of β' given in Table III.

TABLE VI. The same as Table V but for $m = 5$, 6, and 7.

| k	$m = 5$ p, d	k	$m = 6$ p, d	k	$m = 7$ p, d
2	0.957,0.01088	3	0.967,0.00822	3	0.941,0.001464
3	0.989,0.00186	4	0.991,0.0009	4	0.978,0.005134
6	0.995,0.00044	5	0.965,0.00882	5	0.991,0.000112
7	0.987,0.00253	6	0.976,0.00562	6	0.978,0.005358
8	0.981,0.00479	7	0.988,0.00248	7	0.974,0.006416
9	0.996,0.00046	8	0.996,0.00046	8	0.987,0.003019
10	0.990,0.00232	9	0.983,0.00416	9	0.990,0.002234
11	0.990,0.00264	10	0.991,0.00241	10	0.995,0.00096
12	0.996,0.00206	12	0.996,0.00054	15	0.997,0.00094
13	0.996,0.00037	16	0.996,0.00138	20	0.996,0.0013
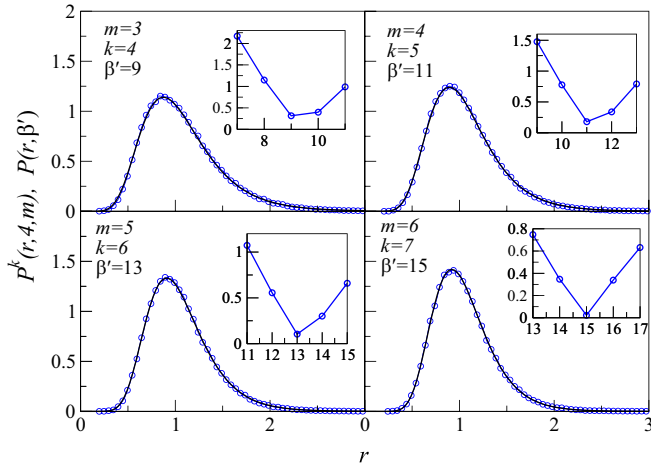
FIG. 15. Distribution of the k-th order spacing ratios (circles) for various values of k and superposition of m CSE spectra. The dimension of the matrices is $N = 1000$. The solid curve corresponds to $P(r, \beta')$ as given in Eq. (1) with β' given in Table IV. The insets show D as a function of β'.

earlier works [21,37,78] in similar kinds of analyses. It can be seen that $D(\beta')$ can take any positive value (upper bound) depending on the range of i in the summation, but is minimum only for that value of β' for which $P(r, \beta')$ is best fit for the observed histogram. The values of k for given m are the same as those in Figs. 1–13, 15, and 16. The results of $D(\beta')$ are shown in the insets of these figures. It can be seen that the minima of $D(\beta')$ in each case coincides remarkably with those of corresponding β' from the main figures. After finding the best fit for the observed data using $D(\beta')$, we go on to check how close the two probability distributions and their respective cumulative functions are. First, the overlap (p) between the probability plots in Figs. 1–13, 15, and 16 is calculated using the following definition:

$$p = 1 - \int \left| P_{\text{obs}}^k(r, \beta, m) - P(r, \beta') \right| dr. \qquad (17)$$

Second, the cumulative distribution functions corresponding to observed data $P_{\text{obs}}^k(r, \beta, m)$ and $P(r, \beta')$ are studied. The maximum absolute difference (d) between these cumulative distributions is calculated using the following definition:

$$d = \sup_{r_i} |F_{\text{obs}}^k(r_i, \beta, m) - F(r_i, \beta')|. \qquad (18)$$

By definition $0 \leqslant p, d \leqslant 1$ and larger (smaller) value of p (d) will indicate that the numerically observed distribution is
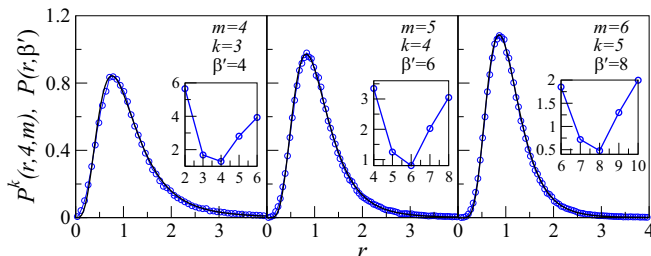

FIG. 16. The same as Fig. 15 but for different values of k and m.

TABLE VII. The same as Table V but for CUE and $m = 3$.

k	$m = 3$ p, d	k	$m = 3$ p, d
3	0.9673,0.008161	9	0.9977,0.0006759
4	0.9965,0.0007662	10	0.9976,0.00080449
5	0.9813,0.005530	11	0.9965,0.0015069
6	0.9948,0.000936	12	0.9961,0.0005231
7	0.9893,0.004329	13	0.9971,0.0011679
8	0.9960,0.0017572	14	0.99709,0.0006004

close to that of the postulated one. Unlike $D(\beta')$, these values will only improve as the range of i is increased. The values are shown in Tables V–XI. Tables V–VIII give strong evidence for our results in Tables II–IV corresponding to the superposition of COE, CUE, and CSE, respectively. In Tables IX–XI results are shown for the physical system of QKT, measured nuclear resonances, and the spin Hamiltonian as plotted in Figs. 6–11. It can be seen that in all cases the values of p and d shown in these tables give strong evidence for our results in these figures. The effect of small sample size in the case of nuclear resonances can be seen in Table X.

VIII. SUMMARY AND CONCLUSIONS

This paper has studied the long-range correlations in the superposed spectra of COE, CUE, and CSE using higher-order spacing ratios. We have given a table for the modified Dyson indices (β') corresponding to the distribution of k-th order spacing ratio when the m number of matrices each from COEs, CUEs, and CSEs is superposed. For the case when two COEs are superposed, two scaling relations relating β' and k are found for even and odd values of k, respectively. The relation corresponding to even k is related to the earlier result on the connection between CUE and the superposition of two COEs at the level of jpdf [22,23]. Conjectures on the lines of Ref. [21] are given. For the case of COE, it is conjectured that for given m, the distribution of the k-th order spacing ratio is related to β' such that the relation $\beta' = k + 1 = m + 2$ for $m \geqslant 2$ and $\beta' = k - 1 = m - 4$ for $m \geqslant 5$ holds true.

TABLE VIII. The same as Table V but for CSE and $m = 4$, 5, and 6.

k	$m = 4$ p, d	k	$m = 5$ p, d	k	$m = 6$ p, d
2	0.9821,0.00884	4	0.9966,0.00657	3	0.9698,0.00709
3	0.9538,0.009765	5	0.9896,0.00114	4	0.9530,0.00870
4	0.9784,0.005174	6	0.9896,0.00216	5	0.9760,0.00540
5	0.9856,0.00353	7	0.9880,0.00209	6	0.9850, 0.00379
6	0.988,0.002077	8	0.9888,0.00247	7	0.9918,0.00129
7	0.9907,0.002545	9	0.9872,0.00272	8	0.9874,0.00298
8	0.9873,0.002881	10	0.9948,0.00132	9	0.9931,0.00100
9	0.9913,0.002375	11	0.9941,0.00114	10	0.9916, 0.00195
10	0.9917,0.001246	12	0.9923,0.00152	11	0.9907, 0.00179
11	0.9938,0.001067			12	0.9897,0.00212
12	0.9636,0.001533				

TABLE IX. The overlap probability p and the maximum absolute difference d for the distribution of higher-order spacing ratios using the eigenvalues of QKT in chaotic case. The value of β' for given k is the same as that in Figs. 6 and 7.

k	β'	p, d	k	β'	p, d
2	2	0.97263,0.003742	8	23	0.97814,0.002949
3	4	0.95997,0.008608	9	28	0.98059,0.002558
4	7	0.97056,0.003950	10	34	0.97707,0.002847
5	10	0.97393,0.004558	11	40	0.97981,0.001904
6	14	0.98118,0.001842	12	47	0.97895,0.004052
7	18	0.97883,0.003812	13	54	0.98250,0.002808

TABLE XI. The overlap probability p and the maximum absolute difference d for the distribution of higher-order spacing ratios using the eigenvalues of spin chains in chaotic case. The value of β' for given k is the same as that in Figs. 9 (left), 10 (right), and 11 (right).

k	β'	p, d	k	β'	p, d
2	2	0.93226,0.01725	2	1	0.92570,0.01059
3	4	0.92965,0.01293	3	2.5	0.95498,0.01021
4	7	0.93976,0.01779	4	4	0.95163,0.00550
5	11	0.92546,0.03858	5	6	0.93557,0.01493
6	12	0.95894,0.00826	6	8	0.93278,0.01389
7	16	0.94367,0.01096	7	10	0.94717,0.01175
			8	12	0.94094,0.00822
			9	16	0.94468,0.01891
			10	17	0.94992,0.00791

Similarly, for the case of CSE, the relation $\beta' = 2k + 1 = 2m + 3$ for $m \geqslant 2$ and $\beta' = 2(k - 1) = 2(m - 2)$ for $m \geqslant 3$ holds true.

We have tested our results on three different physical systems. The first one is the QKT in the quantum chaotic limit belonging to COE. The other two are the measured nuclear resonances and a spin Hamiltonian both corresponding to the GOE. These systems are known to have symmetries. For the case of QKT, we have tested our RMT results of the $m = 2$ case up to $k = 13$ and found very good agreement. This agrees with the earlier analytical result from Ref. [19], where it is shown that its Hamiltonian has two symmetries, whereas in the case of nuclear resonances, we could find agreement only up to $k = 3$ due to nonuniform density as well as small sample size. But the results of $k = 2$ and 3 were enough to conclude the presence of two symmetries using the uniqueness of our tabulated COE results. The third system we considered is the quantum chaotic spin Hamiltonian. Depending on the values of the parameter, a given spin sector can have two or four symmetries. In both the cases we tested our COE results of $m = 2$ and $m = 4$. In this case, we also observed the effects of nonuniform density but at large values of k compared with the previous case due to the large matrix dimension. These results imply that our RMT results hold very well to quantum chaotic physical systems modeled by circular ensembles. For others, we may see the deviations for higher values of k depending on the system and its matrix dimension or the sample size. Despite this we could successfully find the symmetries of systems modeled by Gaussian ensembles. Looking at our results and Refs. [7,8,21,37–39], especially Ref. [37], our results can be claimed to be true for Gaussian ensembles in the limit of large matrix dimensions. Thus, our results can be used to find the symmetries in unknown physical systems.

For the case of $m = 3$ superposition of CUEs, two scaling relations relating β' and k are found for even and odd values

of k. These scaling relations along with other results are confirmed numerically using large matrix dimensions. We have used various numerical tests for the verification of our results. We conjectured that for given m (k), the sequence of β' as a function of k (m) is increasing (decreasing) and is unique to a given circular β-ensemble. As a corollary, finding symmetries as well as whether a given quantum chaotic system is time-reversal invariant (with or without the spin degree of freedom) or not can be found unambiguously. The Gaussian ensembles have been implemented in various experimental systems [110–114]. Thus, our circular ensemble results can be tested using these experiments by taking experimental systems with suitable geometrical symmetry corresponding to given m.

This work has given rise to new future directions as well. We would like to test our results as an additional and stringent test for finding symmetries in various other quantum complex systems [21,25,73]. Various quantum chaotic systems with and without time-reversal invariance and having additional symmetries can be tested. Our study can be extended to the case when matrices of unequal dimensions are superposed, which will be relevant to understanding symmetries in various other spin systems [21,25,115,116]. Our study can be extended to other relevant ensembles from RMT, for example, the ensembles with chiral symmetry [117–123] and Wishart ensemble [4,78,124–126].

TABLE X. The same as Table XI but for the data of nuclear resonances. The value of β' for given k is the same as that in Fig. 8.

k	β'	p, d	k	β'	p, d
2	2	0.88868,0.018197	4	6	0.89450,0.028502
3	4	0.85402,0.027265	5	8	0.87177,0.031754

[1] H. A. Weidenmüller and G. E. Mitchell, Rev. Mod. Phys. **81**, 539 (2009).

[2] G. E. Mitchell, A. Richter, and H. A. Weidenmüller, Rev. Mod. Phys. **82**, 2845 (2010).

[3] F. Haake, *Quantum Signatures of Chaos* (Springer, 3rd Edition, Berlin, 2010).

[4] G. Akemann, J. Baik, and P. Di Francesco, *The Oxford Handbook of Random Matrix Theory* (Oxford University Press, New York, 2011).

[5] H.-J. Stöckmann, *Quantum Chaos: An Introduction* (University Press, Cambridge, 1999).

[6] C. E. Porter, *Statistical Theories of Spectra: Fluctuations* (Academic Press, New York, 1965).

[7] P. J. Forrester, *Log-Gases and Random Matrices* (Princeton University Press, Princeton and Oxford, 2010).

[8] M. L. Mehta, *Random Matrices* (Elsevier Academic Press, 3rd Edition, London, 2004).

[9] T. Guhr, A. Müeller-Groeling, and H. A. Weidenmüeller, Phys. Rep. **299**, 189 (1998).

[10] J. Hutchinson, J. P. Keating, and F. Mezzadri, Phys. Rev. E **92**, 032106 (2015).

[11] H. J. Wells, arXiv:1410.1666 (2014).

[12] W.-J. Rao, Phys. Rev. B **102**, 054202 (2020).

[13] W.-J. Rao, J. Phys. A: Math. Theor. **54**, 105001 (2021).

[14] W.-J. Rao, arXiv:2105.04468 (2021).

[15] J. Gómez, K. Kar, V. Kota, R. A. Molina, A. Relaño, and J. Retamosa, Phys. Rep. **499**, 103 (2011).

[16] O. Bohigas, M. J. Giannoni, and C. Schmit, Phys. Rev. Lett. **52**, 1 (1984).

[17] N. E. Hurt, *Quantum Chaos and Mesoscopic Systems: Mathematical Methods in the Quantum Signatures of Chaos*, vol. 397 (Springer Science & Business Media, 2013).

[18] V. Oganesyan and D. A. Huse, Phys. Rev. B **75**, 155111 (2007).

[19] F. Haake, M. Kus, and R. Scharf, Z. Phys. B **65**, 381 (1987).

[20] L. E. Reichl, *The Transition to Chaos, 2nd edition* (Springer-Verlag, New York, 2004).

[21] S. H. Tekur and M. S. Santhanam, Phys. Rev. Res. **2**, 032063(R) (2020).

[22] F. J. Dyson, J. Math. Phys. **3**, 166 (1962).

[23] J. Gunson, J. Math. Phys. **3**, 752 (1962).

[24] G. W. Anderson, A. Guionnet, and O. Zeitouni, *An Introduction to Random Matrices*, vol. 118 (Cambridge university press, 2010).

[25] O. Giraud, N. Macé, E. Vernier, and F. Alet, arXiv:2008.11173 (2020).

[26] L. F. Santos and M. Rigol, Phys. Rev. E **82**, 031130 (2010).

[27] A. Gubin and L. F. Santos, Am. J. Phys. **80**, 246 (2012).

[28] K. Brading and E. Castellani, *Symmetries in Physics: Philosophical Reflections* (Cambridge University Press, 2003).

[29] S. Corry, *Symmetry and Quantum Mechanics* (Chapman and Hall/CRC, 2016).

[30] D. J. Gross, Proc. Natl. Acad. Sci. **93**, 14256 (1996).

[31] J. Rosen, *Symmetry Rules: How Science and Nature are Founded on Symmetry* (Springer Science & Business Media, 2008).

[32] K. Tapp, *Symmetry: A Mathematical Exploration* (Springer Science & Business Media, 2011).

[33] G. Longo and M. Montévil, *Perspectives on Organisms: Biological Time, Symmetries and Singularities* (Springer Science & Business Media, 2013).

[34] G. Sardanashvily, *Noether's Theorems* (Springer, 2016).

[35] Y. Kosmann-Schwarzbach, *The Noether Theorems* (Springer, 2011), pp. 55–64.

[36] J. S. Cotler, G. Gur-Ari, M. Hanada, J. Polchinski, P. Saad, S. H. Shenker, D. Stanford, A. Streicher, and M. Tezuka, J. High Energy Phys. **2017**, 118 (2017).

[37] S. H. Tekur, U. T. Bhosale, and M. S. Santhanam, Phys. Rev. B **98**, 104305 (2018).

[38] C. E. Porter, Nucl. Phys. **40**, 167 (1963).

[39] P. B. Kahn and C. E. Porter, Nucl. Phys. **48**, 385 (1963).

[40] I. Dumitriu and A. Edelman, J. Math. Phys. **43**, 5830 (2002).

[41] W. Buijsman, V. Cheianov, and V. Gritsev, Phys. Rev. Lett. **122**, 180601 (2019).

[42] P. Sierant and J. Zakrzewski, Phys. Rev. B **99**, 104205 (2019).

[43] M. V. Berry, Proc. R. Soc. A **400**, 229 (1985).

[44] M. Sieber and K. Richter, Phys. Scr. **2001**, 128 (2001).

[45] S. Müller, S. Heusler, A. Altland, P. Braun, and F. Haake, New J. Phys. **11**, 103025 (2009).

[46] T. Tkocz, M. Smaczyński, M. Kuś, O. Zeitouni, and K. Życzkowski, Random Matrices: Theor. Appl. **1**, 1250009 (2012).

[47] M. Smaczyński, T. Tkocz, M. Kuś, and K. Życzkowski, Phys. Rev. E **88**, 052902 (2013).

[48] T. Tkocz *et al.*, Electron. Commun. Probab. **18**, 1 (2013).

[49] M. V. Berry and M. Tabor, Proc. R. Soc. Lond. A **356**, 375 (1977).

[50] F. J. Dyson, J. Math. Phys. **3**, 140 (1962).

[51] F. Mezzadri, Notices of the AMS **54**, 592 (2007).

[52] R. Killip and I. Nenciu, Inter. Math. Res. Notices **2004**, 2665 (2004).

[53] M. L. Mehta and F. J. Dyson, J. Math. Phys. **4**, 713 (1963).

[54] H. Bruus and J.-C. Angl'es d'Auriac, Phys. Rev. B **55**, 9142 (1997).

[55] J. M. G. Gómez, R. A. Molina, A. Relaño, and J. Retamosa, Phys. Rev. E **66**, 036209 (2002).

[56] Y. Y. Atas, E. Bogomolny, O. Giraud, and G. Roux, Phys. Rev. Lett. **110**, 084101 (2013).

[57] Y. Atas, E. Bogomolny, O. Giraud, P. Vivo, and E. Vivo, J. Phys. A: Math. Theor. **46**, 355204 (2013).

[58] V. Oganesyan, A. Pal, and D. A. Huse, Phys. Rev. B **80**, 115104 (2009).

[59] A. Pal and D. A. Huse, Phys. Rev. B **82**, 174411 (2010).

[60] S. Iyer, V. Oganesyan, G. Refael, and D. A. Huse, Phys. Rev. B **87**, 134202 (2013).

[61] E. Cuevas, M. Feigel'Man, L. Ioffe, and M. Mezard, Nat. Commun. **3**, 1128 (2012).

[62] G. Biroli, A. Ribeiro-Teixeira, and M. Tarzia, arXiv:1211.7334 (2012).

[63] C. Chen, F. Burnell, and A. Chandran, Phys. Rev. Lett. **121**, 085701 (2018).

[64] L. F. Santos and M. Rigol, Phys. Rev. E **81**, 036206 (2010).

[65] C. Kollath, G. Roux, G. Biroli, and A. M. Läuchli, J. Stat. Mech.: Theory Exp. (2010) P08011.

[66] M. Rigol and L. F. Santos, Phys. Rev. A **82**, 011604(R) (2010).

[67] M. Collura, H. Aufderheide, G. Roux, and D. Karevski, Phys. Rev. A **86**, 013615 (2012).

[68] E. Tarquini, G. Biroli, and M. Tarzia, Phys. Rev. Lett. **116**, 010601 (2016).

[69] A. L. Corps and A. Relaño, Phys. Rev. E **101**, 022222 (2020).

[70] F. Sun and J. Ye, Phys. Rev. Lett. **124**, 244101 (2020).

[71] F. Sun, Y. Yi-Xiang, J. Ye, and W.-M. Liu, Phys. Rev. D **101**, 026009 (2020).

[72] T. Nosaka and T. Numasawa, J. High Energy Phys. 08 (2020) 081.

[73] M. Srdinsek, T. Prosen, and S. Sotiriadis, Phys. Rev. Lett. **126**, 121602 (2021).

[74] N. Chavda, H. Deota, and V. Kota, Phys. Lett. A **378**, 3012 (2014).

[75] V. Kota and N. Chavda, Int. J. Mod. Phys. E **27**, 1830001 (2018).

[76] S. H. Tekur, S. Kumar, and M. S. Santhanam, Phys. Rev. E **97**, 062212 (2018).

[77] L. Sá, P. Ribeiro, and T. Prosen, Phys. Rev. X **10**, 021019 (2020).

[78] U. T. Bhosale, S. H. Tekur, and M. S. Santhanam, Phys. Rev. E **98**, 052133 (2018).

[79] P. Rao, M. Vyas, and N. D. Chavda, Eur. Phys. J. Special Topics **229**, 2603 (2020).

[80] T. A. Brody, J. Flores, J. B. French, P. A. Mello, A. Pandey, and S. S. M. Wong, Rev. Mod. Phys. **53**, 385 (1981).

[81] A. Y. Abul-Magd and M. H. Simbel, Phys. Rev. E **60**, 5371 (1999).

[82] N. M. Katz and P. Sarnak, Bull. Am. Math. **36**, 1 (1999).

[83] J. P. Keating and N. C. Snaith, J. Phys. A: Math. Gen. **36**, 2859 (2003).

[84] W.-J. Rao and M. Chen, Eur. Phys. J. Plus **136**, 81 (2021).

[85] P. J. Forrester and E. M. Rains, Probab. Theory Relat. Fields **130**, 518 (2004).

[86] P. J. Forrester, Commun. Math. Phys. **285**, 653 (2009).

[87] U. T. Bhosale, arXiv:1905.02585 (2019).

[88] J. Zakrzewski and M. Kuś, Phys. Rev. Lett. **67**, 2749 (1991).

[89] R. Alicki, D. Makowiec, and W. Miklaszewski, Phys. Rev. Lett. **77**, 838 (1996).

[90] Y. S. Weinstein, S. Lloyd, and C. Tsallis, Phys. Rev. Lett. **89**, 214101 (2002).

[91] R. Demkowicz-Dobrzański and M. Kuś, Phys. Rev. E **70**, 066216 (2004).

[92] S. Chaudhury, A. Smith, B. E. Anderson, S. Ghose, and P. S. Jessen, Nature **461**, 768 (2009).

[93] M. Lombardi and A. Matzkin, Phys. Rev. E **83**, 016207 (2011).

[94] Z. Puchała, L. Pawela, and K. Życzkowski, Phys. Rev. A **93**, 062112 (2016).

[95] C. Neill, P. Roushan, M. Fang, Y. Chen, M. Kolodrubetz, Z. Chen, A. Megrant, R. Barends, B. Campbell, B. Chiaro *et al.*, Nat. Phys. **12**, 1037 (2016).

[96] U. T. Bhosale and M. S. Santhanam, Phys. Rev. E **95**, 012216 (2017).

[97] J. B. Ruebeck, J. Lin, and A. K. Pattanayak, Phys. Rev. E **95**, 062222 (2017).

[98] U. T. Bhosale and M. S. Santhanam, Phys. Rev. E **98**, 052228 (2018).

[99] V. R. Krithika, V. S. Anjusha, U. T. Bhosale, and T. S. Mahesh, Phys. Rev. E **99**, 032219 (2019).

[100] E. J. Meier, J. Ang'ong'a, F. A. An, and B. Gadway, Phys. Rev. A **100**, 013623 (2019).

[101] M. H. Muñoz Arias, P. M. Poggi, P. S. Jessen, and I. H. Deutsch, Phys. Rev. Lett. **124**, 110503 (2020).

[102] T. Xu, T. Scaffidi, and X. Cao, Phys. Rev. Lett. **124**, 140602 (2020).

[103] S. Kumar, Phys. Rev. A **102**, 012405 (2020).

[104] P. A. Miller and S. Sarkar, Phys. Rev. E **60**, 1542 (1999).

[105] G. Hacken, R. Werbin, and J. Rainwater, Phys. Rev. C **17**, 43 (1978).

[106] T. C. Hsu and J. C. Angle's d'Auriac, Phys. Rev. B **47**, 14291 (1993).

[107] L. F. Santos, J. Math. Phys. **50**, 095211 (2009).

[108] K. Kudo and T. Deguchi, J. Phys. Soc. Jpn. **74**, 1992 (2005).

[109] K. Zyczkowski, *Chaos-The Interplay Between Stochastic and Deterministic Behaviour* (Springer, 1995), pp. 565–571.

[110] H. Alt, H.-D. Gräf, T. Guhr, H. L. Harney, R. Hofferbert, H. Rehfeld, A. Richter, and P. Schardt, Phys. Rev. E **55**, 6674 (1997).

[111] C. Dembowski, H.-D. Gräf, A. Heine, H. Rehfeld, A. Richter, and C. Schmit, Phys. Rev. E **62**, R4516 (2000).

[112] R. Schäfer, M. Barth, F. Leyvraz, M. Müller, T. H. Seligman, and H.-J. Stöckmann, Phys. Rev. E **66**, 016202 (2002).

[113] B. Dietz, T. Guhr, B. Gutkin, M. Miski-Oglu, and A. Richter, Phys. Rev. E **90**, 022903 (2014).

[114] A. Rehemanjiang, M. Allgaier, C. H. Joyner, S. Müller, M. Sieber, U. Kuhl, and H.-J. Stöckmann, Phys. Rev. Lett. **117**, 064101 (2016).

[115] K. Binder and A. P. Young, Rev. Mod. Phys. **58**, 801 (1986).

[116] I. Amico, R. Fazio, A. Osterloh, and V. Vedral, Rev. Mod. Phys. **80**, 517 (2008).

[117] Y. V. Fyodorov and E. Strahov, Nucl. Phys. B **647**, 581 (2002).

[118] P. H. Damgaard, J. Phys.: Conf. Ser. **287**, 012004 (2011).

[119] V. Kaymak, M. Kieburg, and T. Guhr, J. Phys. A: Math. Theor. **47**, 295201 (2014).

[120] C. W. J. Beenakker, Rev. Mod. Phys. **87**, 1037 (2015).

[121] G. Akemann, *Stochastic Processes and Random Matrices: Lecture Notes of the Les Houches Summer School* (Oxford University Press, Oxford, 2018), Vol. 104, p. 228.

[122] T. Mondal and P. Shukla, Phys. Rev. E **102**, 032131 (2020).

[123] A. Rehemanjiang, M. Richter, U. Kuhl, and H.-J. Stöckmann, Phys. Rev. Lett. **124**, 116801 (2020).

[124] J. Wishart, Biometrika **20A**, 32 (1928).

[125] S. N. Majumdar and M. Vergassola, Phys. Rev. Lett. **102**, 060601 (2009).

[126] M. Fridman, R. Pugatch, M. Nixon, A. A. Friesem, and N. Davidson, Phys. Rev. E **85**, 020101(R) (2012).